Geometric Modeling and Visualization

http://www.cs.utexas.edu/~bajaj/cs384R08/

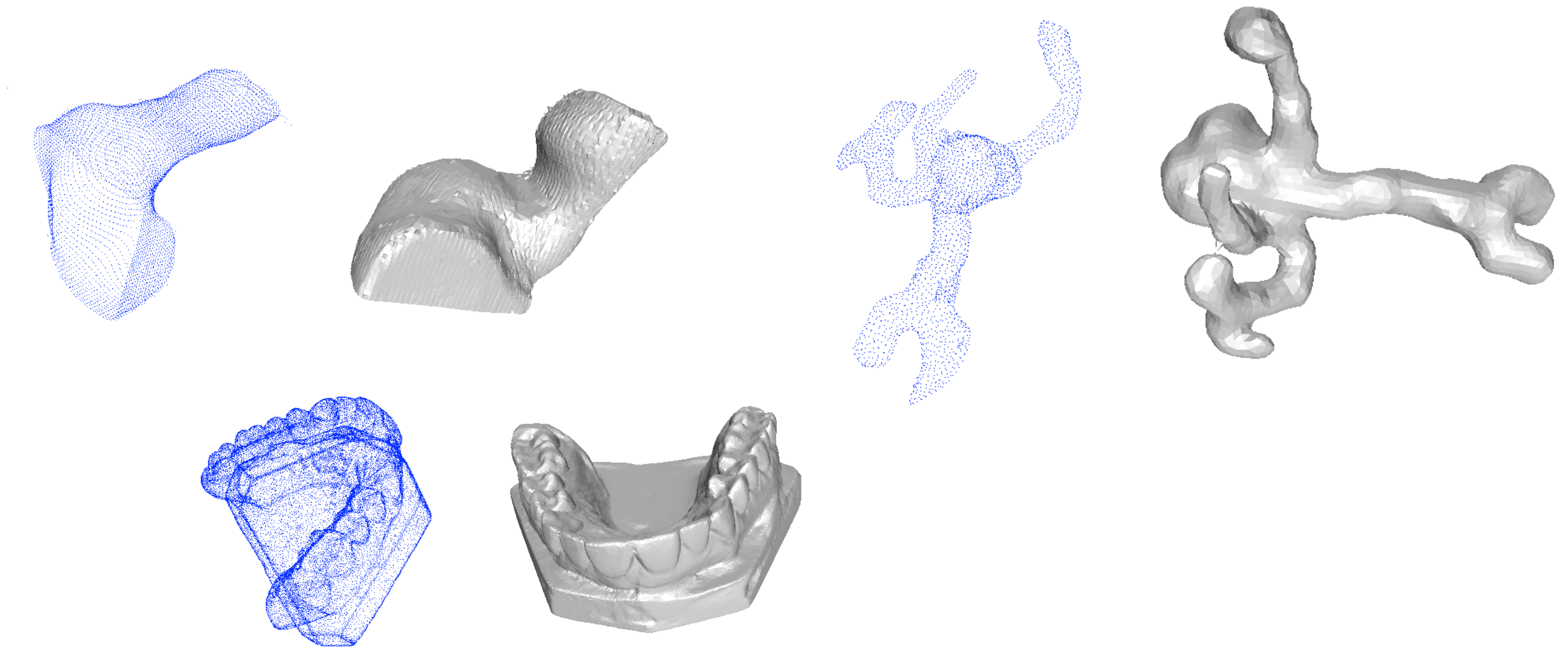

Lecture 6

Structure Reconstruction: Shape Segmentation

Computational Visualization Center
Institute of Computational and Engineering Sciences
Department of Computer Sciences
University of Texas at Austin

September 2008

Patient Specific Heart Models

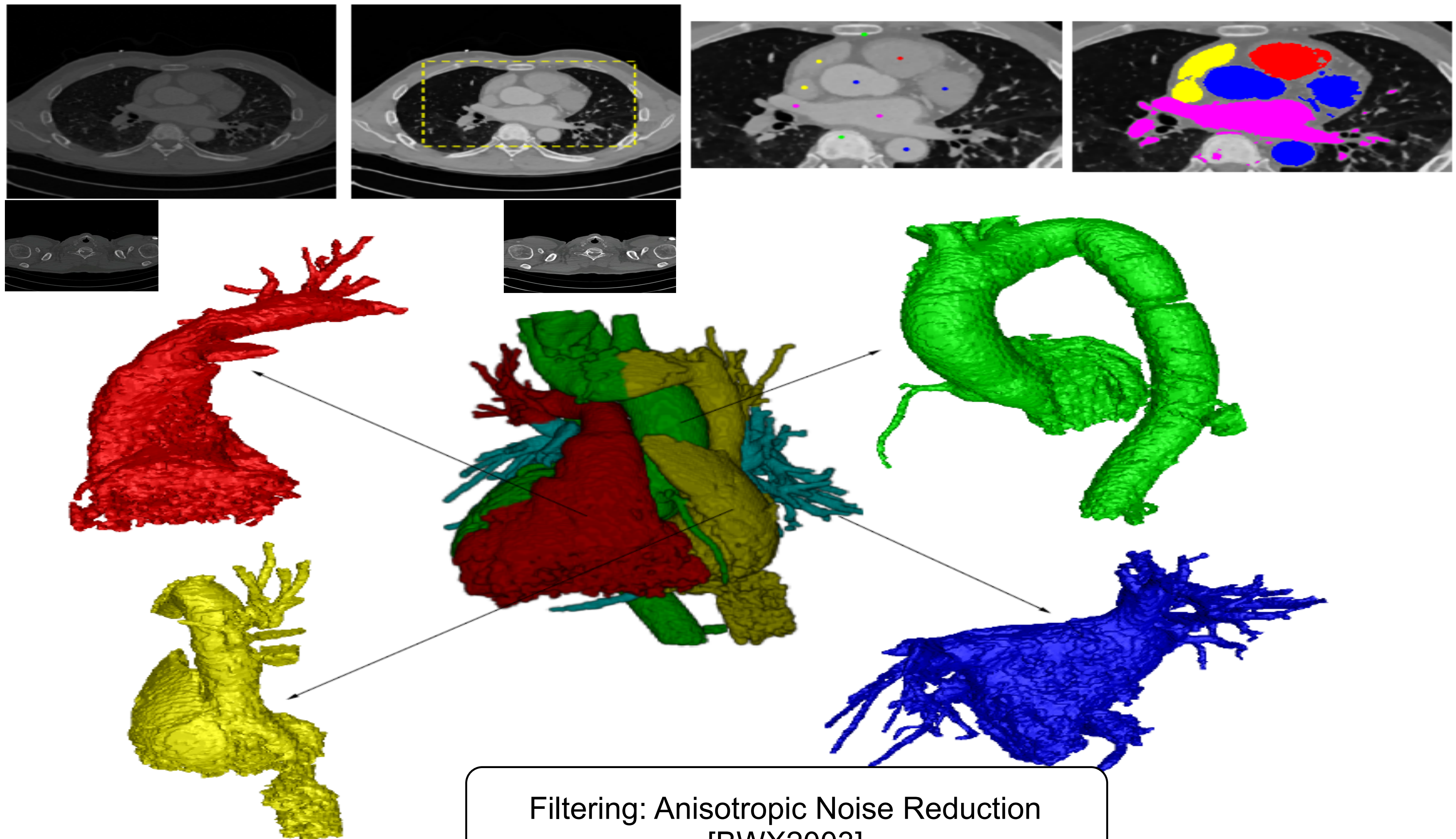

Filtering: Anisotropic Noise Reduction [BWX2003]

Contrast Enhancement: Local Adaptive Intensity Modulation [YB2004]

Segmentation: Multi-seeded FMM [YB2005]

Model Reconstruction from Regularized Voxel Centers (Point Clouds)

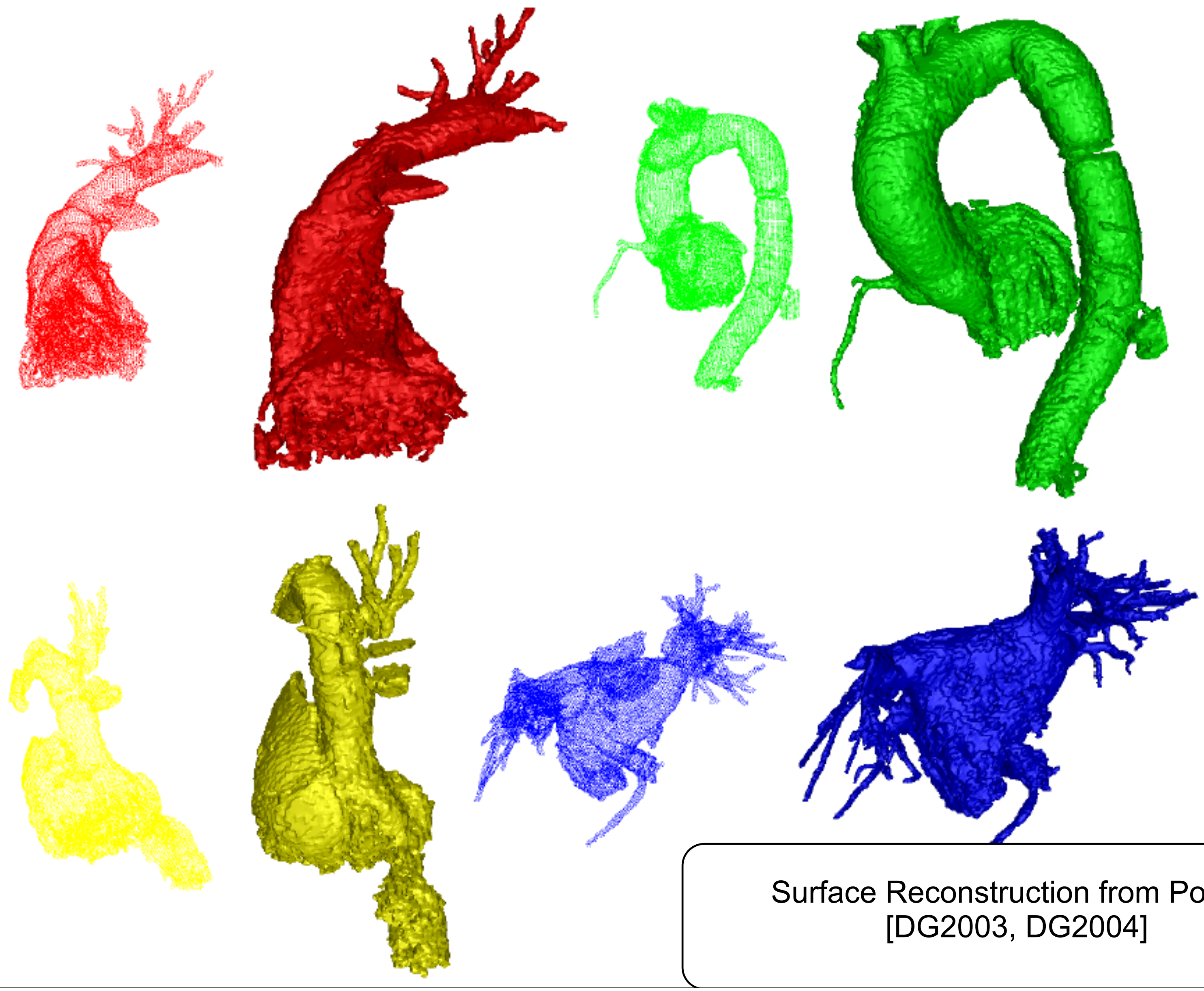

Surface Reconstruction from Points:
[DG2003, DG2004]

Problem Description – Surface and Medial Axis construction

Scanning

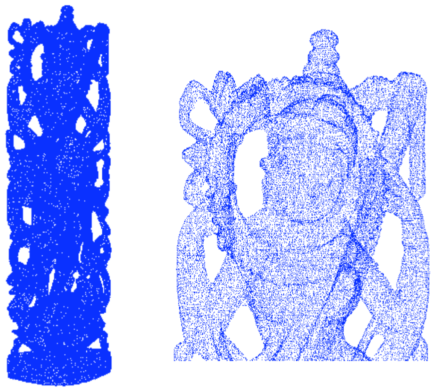

Point Sample with closeup

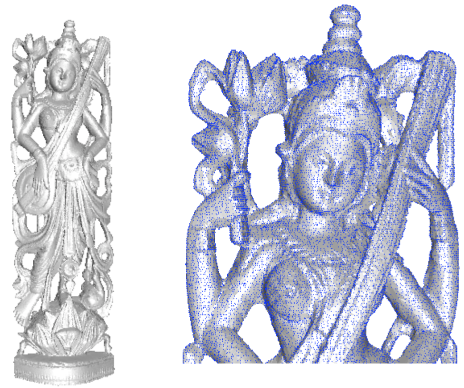

Reconstruction with closeup

Surface Reconstruction Problem:
Given a set of points P sampled from S, create an approximation of S and an approximation of the medial axis of S.

Medial Axis Transform (MAT) Problem:
Given a set of points P sampled from S, create an approximation of M of the medial axis of S.

Medial Axis and Sampling Density

Medial Axis M of a shape S is defined as a set of points which has more than one nearest point on S.

2D Illustration

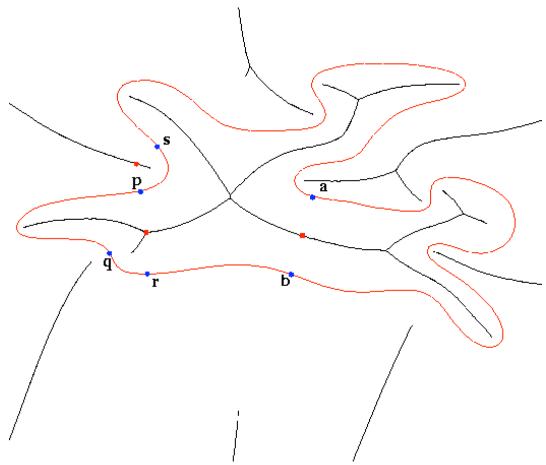

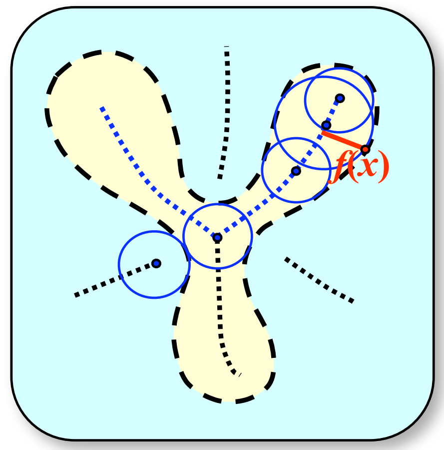

Distance Function h_S assigns every point x the nearest distance to S.

Approximation of h_S is done via h_P when S is known only via a finite set of points P on S.

$$h_P \ : \ \mathbb{R}^3 \to \mathbb{R}, \ \ x \mapsto \min_{p \in P} \|x - p\|$$

Local Feature Size: Distance of a point x on surface to the medial axis. Denoted as $f(x)$.

ε-sampling: Every point on the surface has a sample point p within $\varepsilon f(x)$.

Computational Aspects: Vor/Del of P

Voronoi diagram

$$V_p = \{x \in \mathbb{R}^3 : \forall q \in P - \{p\}, \|x-p\| \leq \|x-q\|)\}$$

Delaunay triangulation

Dual of Voronoi diagram.

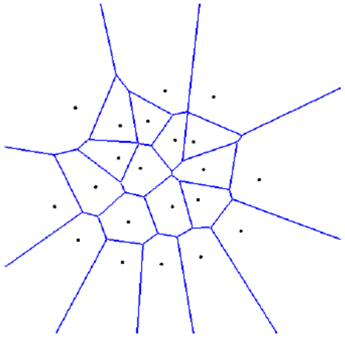

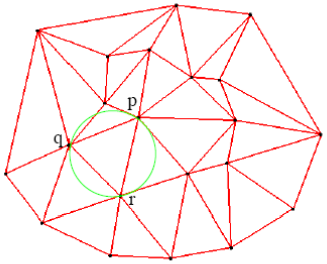

Restricted Voronoi-Delaunay

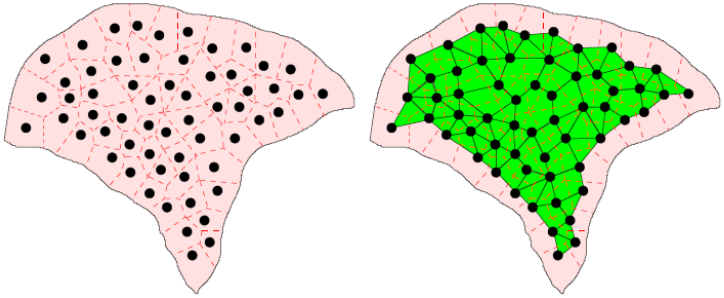

Theory

What is a *correct* reconstruction?

The reconstructed surface is homeomorphic to the original surface and within a small Hausdorff distance.

Theorem [ES1994]

If the Voronoi diagram of sample points satisfies *ball-property,* the restricted Delaunay triangulation is *homeomorphic* to the surface.

What relation does Medial Axis have with the object? [Lieutier2004]

The medial axis is *homotopy equivalent* to the surface.

Ball Property: A k-dimensional Voronoi face intersects the surface in k-1 dimensional ball

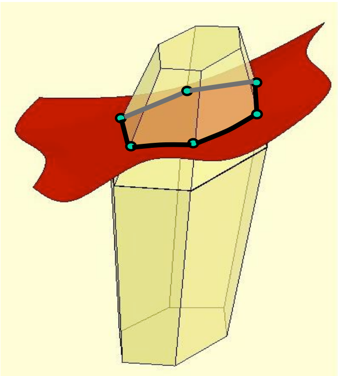

Cocone Family – Cocone, TightCocone, RobustCocone and Medial

Cocone:
Given a set of points P sampled from S, create an approximation of S. Additionally detects the undersampling present in the data.
[Amenta, Choi, Dey, Leekha 2002 – IJCGA]

TightCocone:
Given a set of points P sampled from S, create a watertight approximation of S.
[Dey, Goswami 2003 – ACM Solid Modeling]

RobustCocone:
Given a set of (noisy) points P sampled from or near S, create a watertight approximation of S.
[Dey, Goswami 2004 – ACM SoCG]

Medial Axis Transform:
Given a set of points P sampled from S, approximate the medial axis of S.
[Dey, Zhao 2003 – Algorithmica]

Cocone with Undersampling Detection

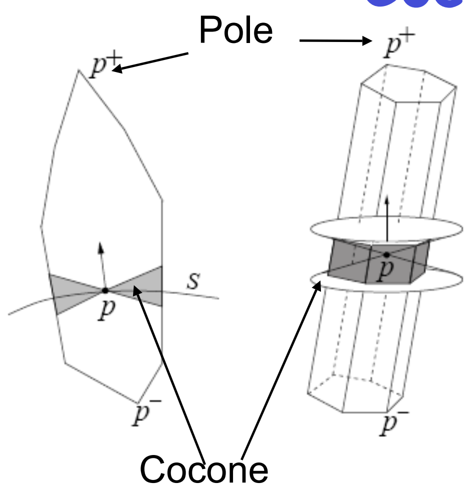

Pole: Furthest Voronoi vertex in the Voronoi cell of a point p.

Vector v_p denotes the vector from p to the pole. This estimates the normal at p.

Cocone: The set $C_p = \{y \in V_p : \angle((y-p), \mathbf{v}_p) \geq \frac{3\pi}{8}\}$ is called the cocone of p.

Algorithm:

Cocone estimates the tangent plane.

1. Compute Delaunay of P
2. Compute *pole* at every p. (Poles approximate normals)
3. Select set of Delaunay triangles incident at p that fall within Cocone of p. Call them *candidate* triangles.
4. Extract the surface from the *candidate* triangles by collecting the outer layer.

Theorem: Reconstructed surface is *homeomorphic* to *S* if *P* is an ε sample of *S* with ε < 0.06.

Results

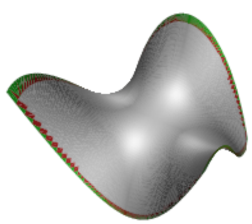

Undersampling - TightCocone

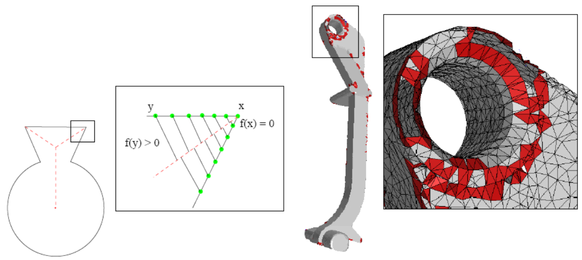

(a) (b)

Marking : Any point whose neighborhood on the initial reconstructed surface is a disk, separates the incident tetrahedra into *IN* and *OUT*.
Goal is to propagate the marking consistently.

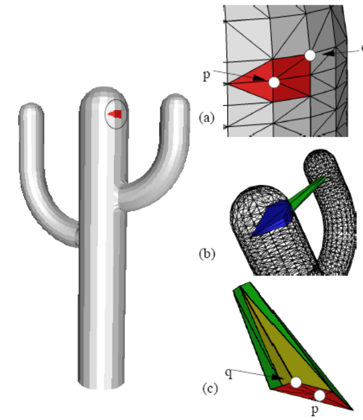

Problem : Medial Axis passes through sharp corners. Feature size = 0. Requires infinite sampling to satisfy sampling density condition.

Peeling : Starting from convex hull, ``walk'' among the *OUT* tetrahedra to sculpt them away leaving the set of *IN* tetrahedra whose boundary is the surface.

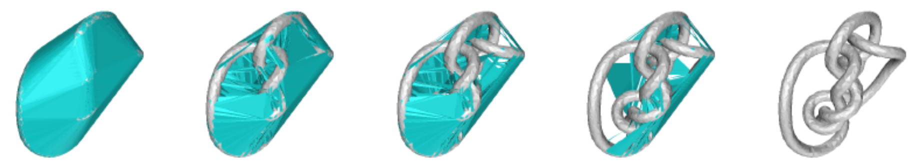

Results

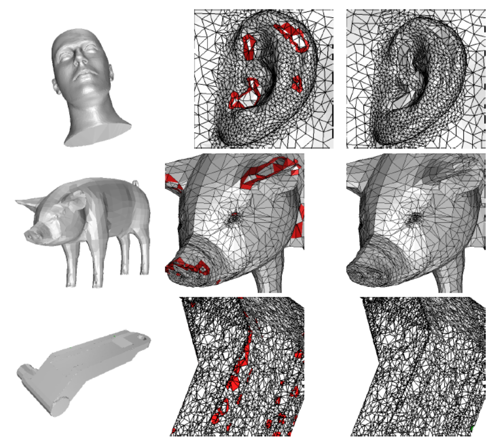

Algorithm

1. Compute initial surface using Cocone.
2. Marking: Around every point with manifold neighborhood, mark the tetrahedra *IN* and *OUT*.
3. Peeling: Starting from convex hull, *peel* all *OUT* tetrahedra.

Noisy Sample - RobustCocone

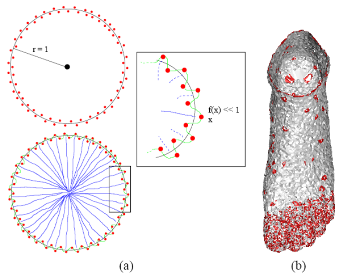

Problem

Big Delaunay Ball

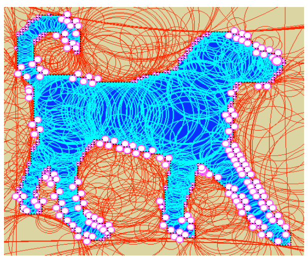

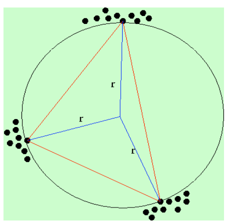

Observation: Noise creates *small* bubbles (pink) near surface. Goal is to remove them.

Algorithm:

1. Identify the *big* Delaunay balls.
2. Separate the *IN* and *OUT* balls.
3. Output the boundary of the union.

Pipeline

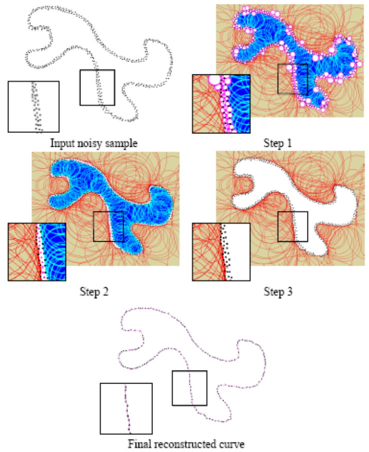

Noisy (ε, κ)-sample

1. $\tilde{P}$ is an ε-sample of Σ.
2. $\|p - \tilde{p}\| \leq k_1 \varepsilon f(\tilde{p})$
3. $\|p - q\| \leq k_2 \varepsilon f(\tilde{p})$

   q is κ-th nearest sample

Projection of the samples on the surface is a dense sample.

The samples are not too far away from the surface.

Any two sample points can not come arbitrarily close.

Noise Model

Theorem:

Boundary of the *big* Delaunay balls is homeomorphic to the surface.

Noisy Horse

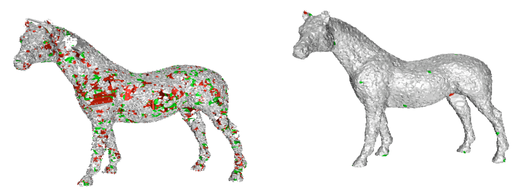

Reconstruction from Volumetric Point Sample

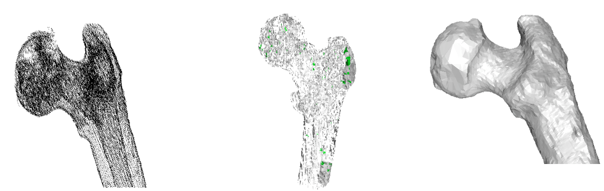

Center for Computational Visualization
Institute of Computational and Engineering Sciences
Department of Computer Sciences
University of Texas at Austin

Point Cloud Reconstruction Examples - BioMed

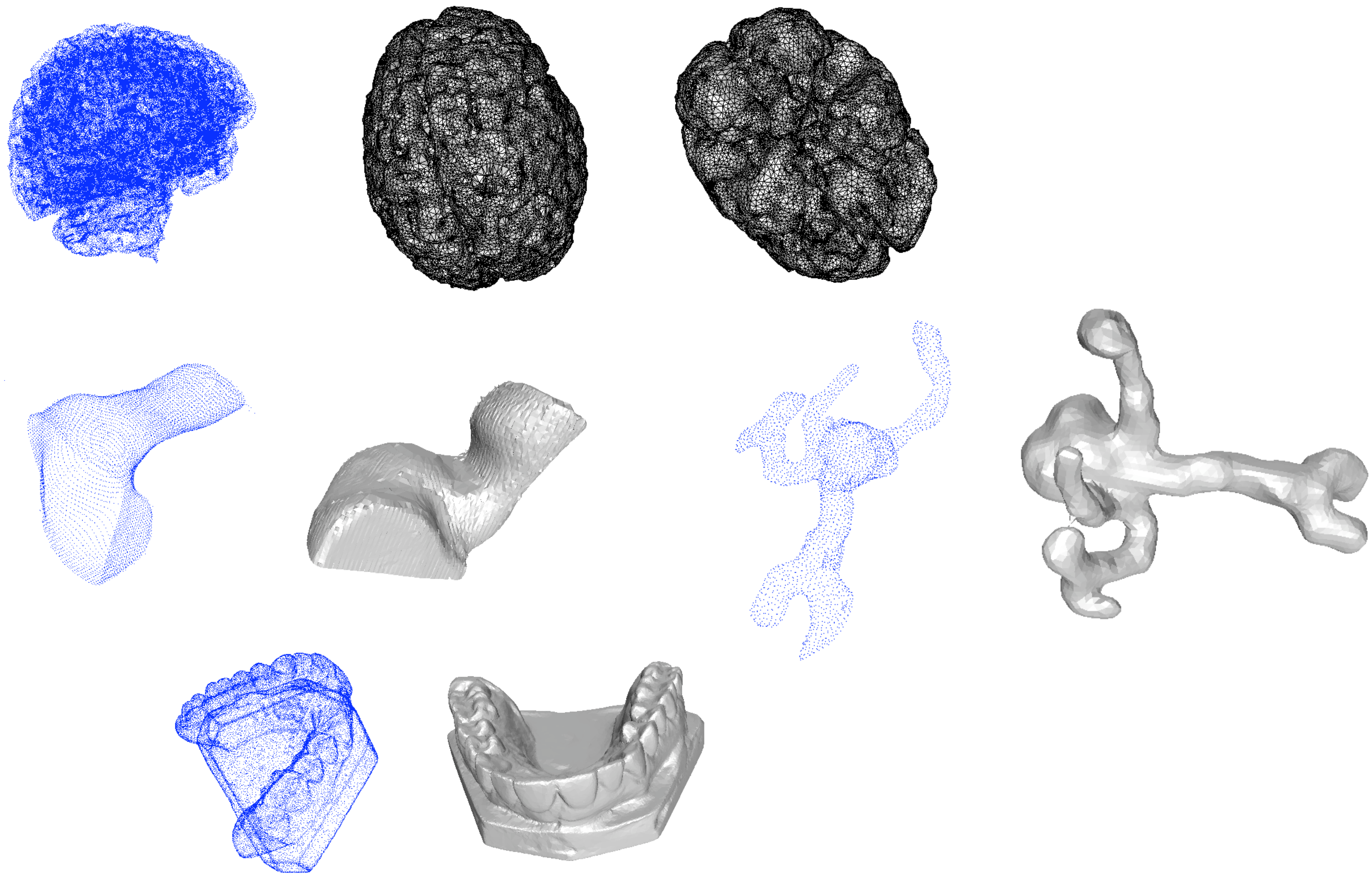

Center for Computational Visualization
Institute of Computational and Engineering Sciences
Department of Computer Sciences
University of Texas at Austin

Medial Axis Approximation

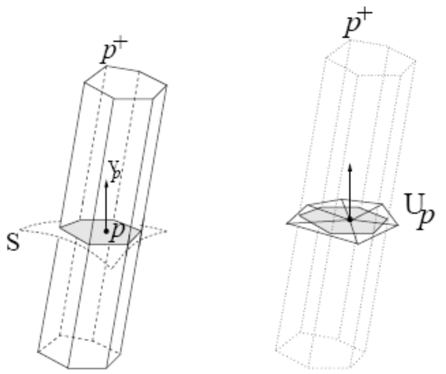

(a) (b)

Umbrella: The plane normal to the pole vector intersects some of the Voronoi edges. Dual Del triangles to those edges form the Umbrella at p.

Angle Condition (θ): Edge *pq* satisfies angle condition if it makes large angle with all the umbrella triangles at *p* and *q*.

Ratio Condition (ρ): Length of *pq* is larger than (ρ times) the circumradius of the umbrella triangles at p and q.

Algorithm

1. Compute Vor-Del of P.
2. Collect all the Voronoi facets whose dual Delaunay edges satisfy both *angle* and *ratio* condition.

Results

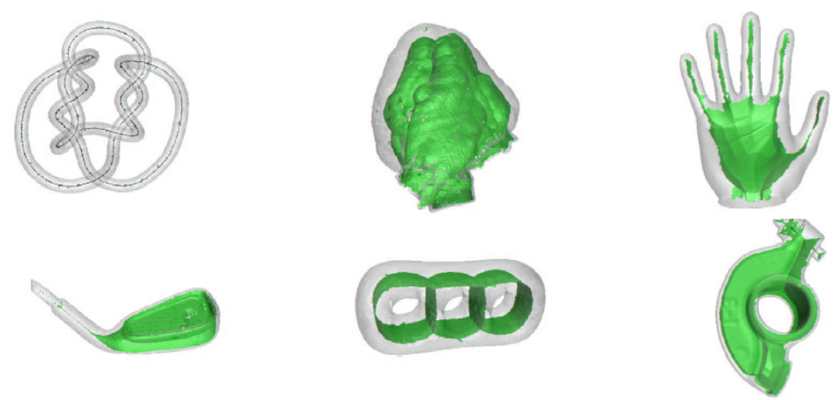

Results of Medial Axis Classification and Curation

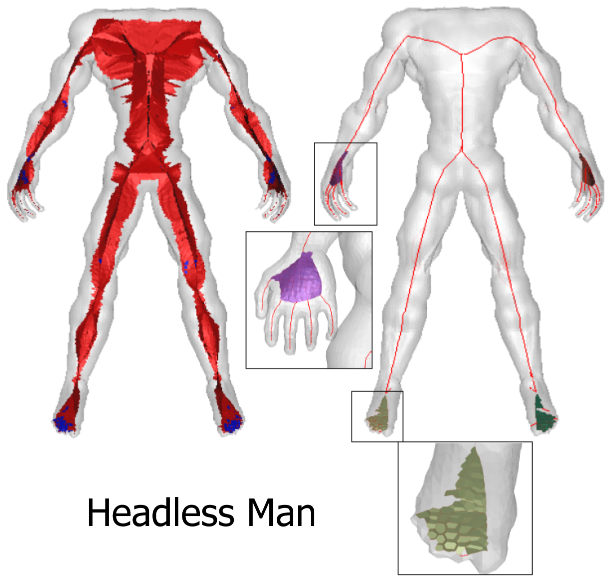

Headless Man

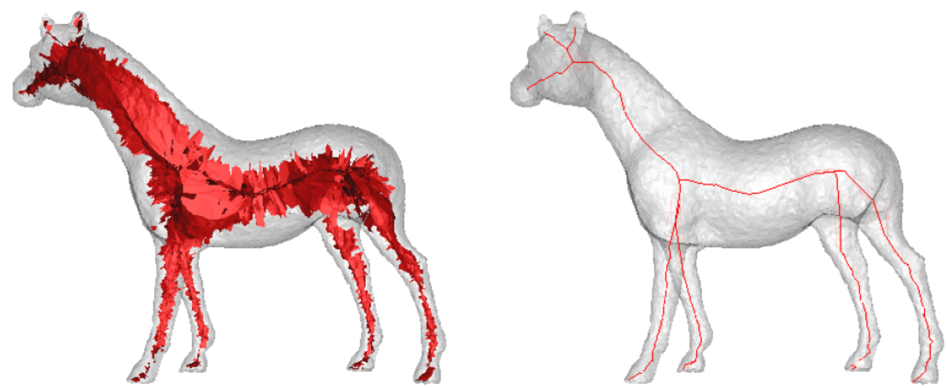

Noisy Horse

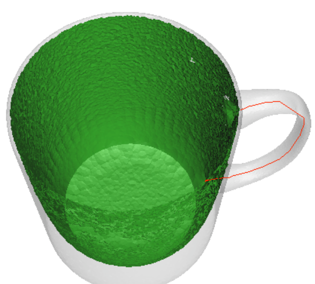

Mug

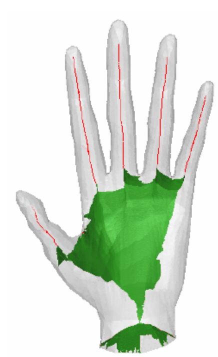

Hand

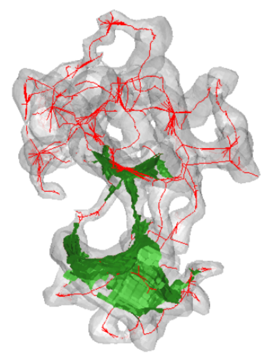

1IRK – 8A

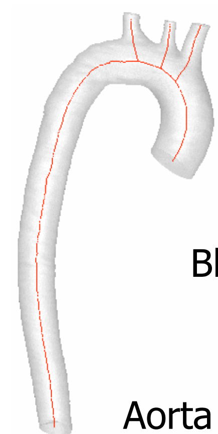

Aorta

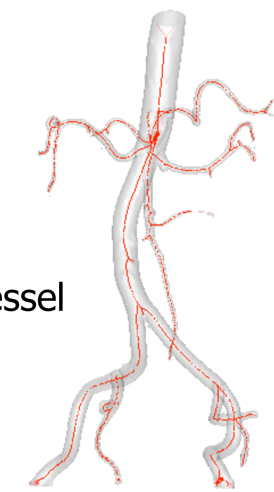

Blood Vessel

Classification of Medial Axis

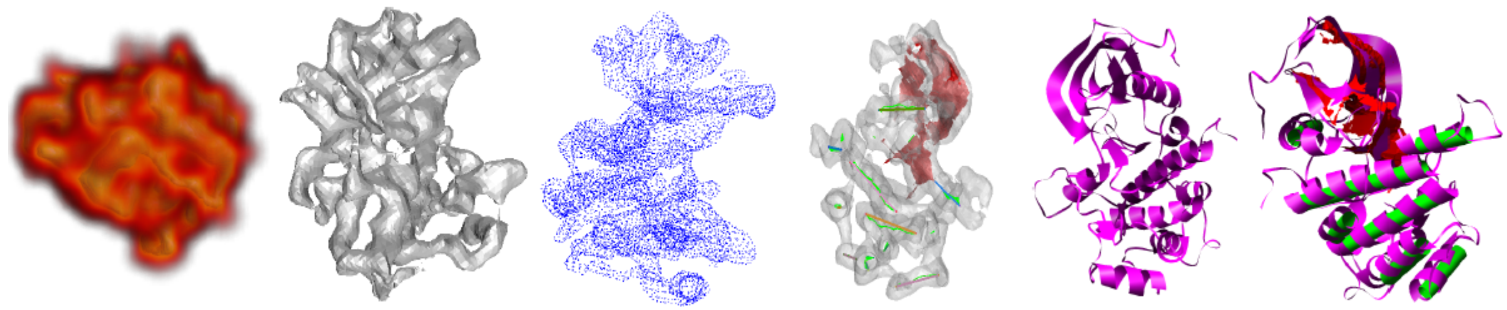

Step 1: Vor/Del(P) computation (using *CGAL*).

Goswami,Dey, Bajaj, ICVGIP'2006

Step 2: Identification of Interior Medial Axis M.

Step 3:

3.a: Identification of Critical points of distance function from Vor/Del(P).

3.b: Selection of Critical points only on M.

[By DGRS2005, Critical points are either near S or near M]

Step 4: Classification of Medial Axis via

4.a: U_1 – Unstable Manifold of index 1 saddle point on M

4.b: U_2 – Unstable Manifold of index 2 saddle point on M.

Step 5: Width Test to select the subsets of U_1 (β-sheets) and U_2 (α-helices).

Critical Points, their Indices, and their Manifolds

Critical Point of a smooth function is a point where the gradient of the function vanishes.

Index of a critical point is the number of independent directions in which the function decreases.

In 3D, four types of critical points

1. Minima – index 0
2. Saddle of index 1
3. Saddle of index 2
4. Maxima – index 3

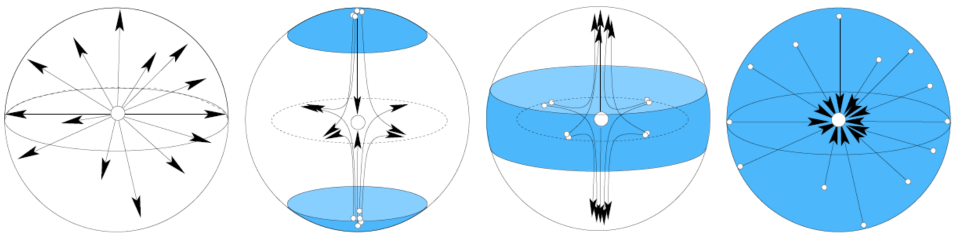

From EHNP SoCG'03

Integral curve : A path in the domain of the function on which at every point the tangent to the curve equals the gradient of the function.

Stable Manifold of a critical point is the union of all integral curves ending at the critical point.

Unstable Manifold of a critical point is the union of all integral curves starting at the critical point.

Vor/Del of P and Critical Points of h_P

Voronoi diagram

$$V_p = \{x \in \mathbb{R}^3 : \forall q \in P - \{p\}, \|x-p\| \le \|x-q\|\}$$

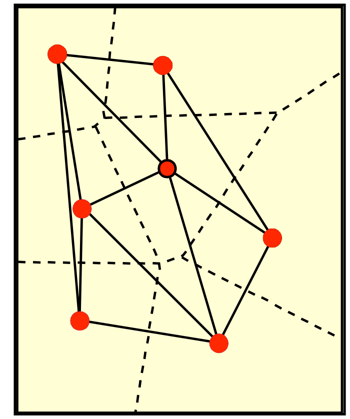

Delaunay triangulation

Dual of Voronoi diagram.

Critical points of h_P can be computed from the Vor/Del(P). These are the intersection of Voronoi and their dual Delaunay objects.

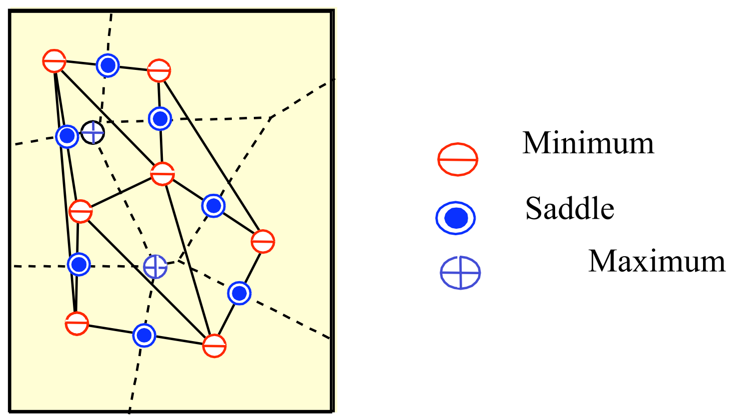

Siersma et al.

Computation of U_2

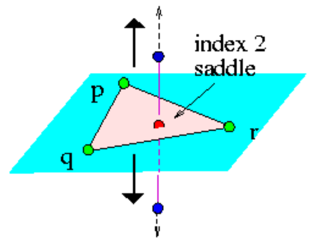

Start

• Start from an index-2 saddle point.

• Generic step: Once reaching a VV, decide if the flow goes through a VE or if it enters a VF.

• Terminate at a local maximum.

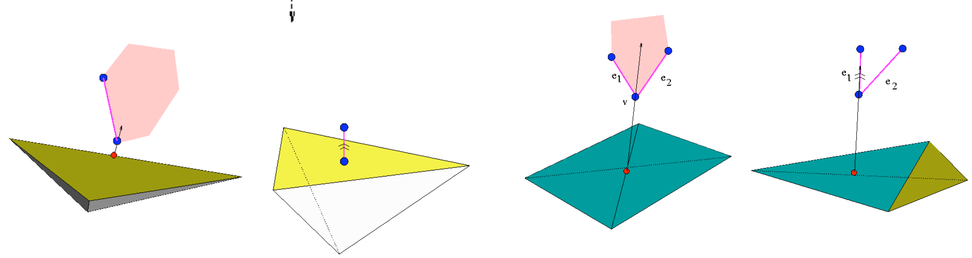

Generic Step

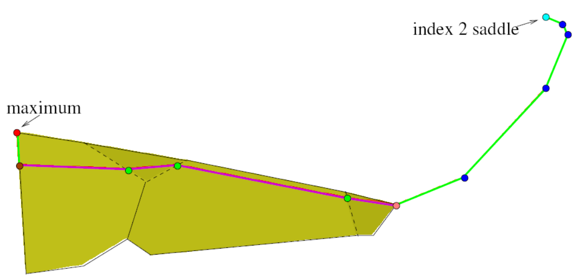

Structure of U_2

Part of U_2 along Voronoi edge

Part of U_2 through Voronoi facets

Voronoi vertex on U_2

Non-Voronoi vertex on U_2

Computation of U_1

- Start from the VF containing an index-1 saddle point.

- Generic step: Identify the VE s on the boundary which are active. Expand the unstable manifold by collecting their acceptor VF s.

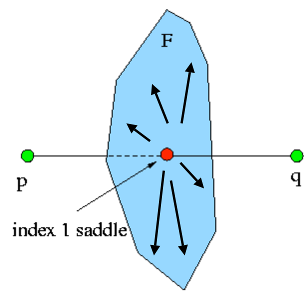

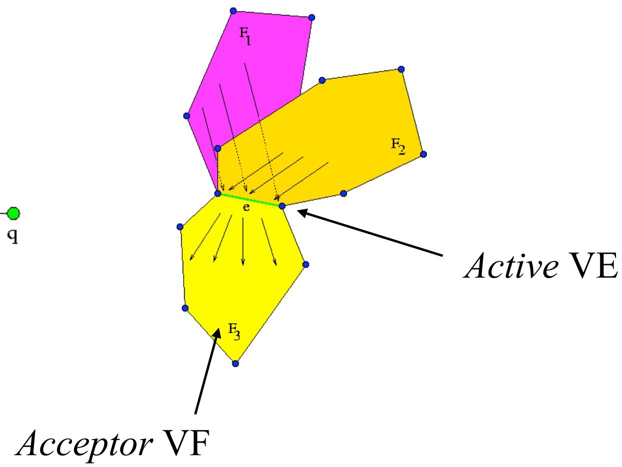

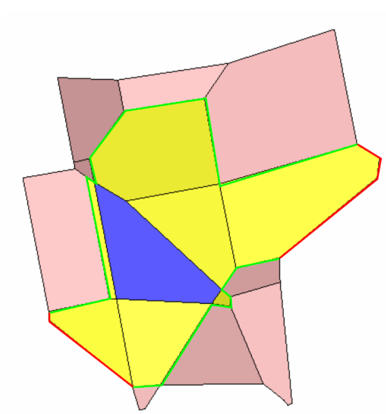

Active Voronoi edges to extend U_1

Passive Voronoi edges defining the boundary of U_1

Secondary Structure of RDV Outer Capsid Coat Protein P8

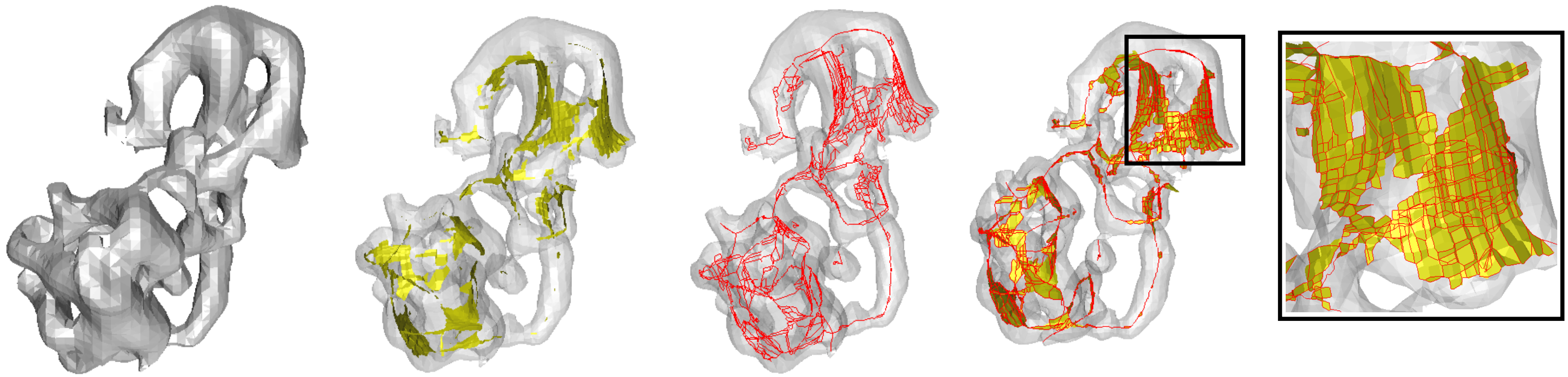

Surface | U_1 | U_2 | U_1 and U_2 | Closeup

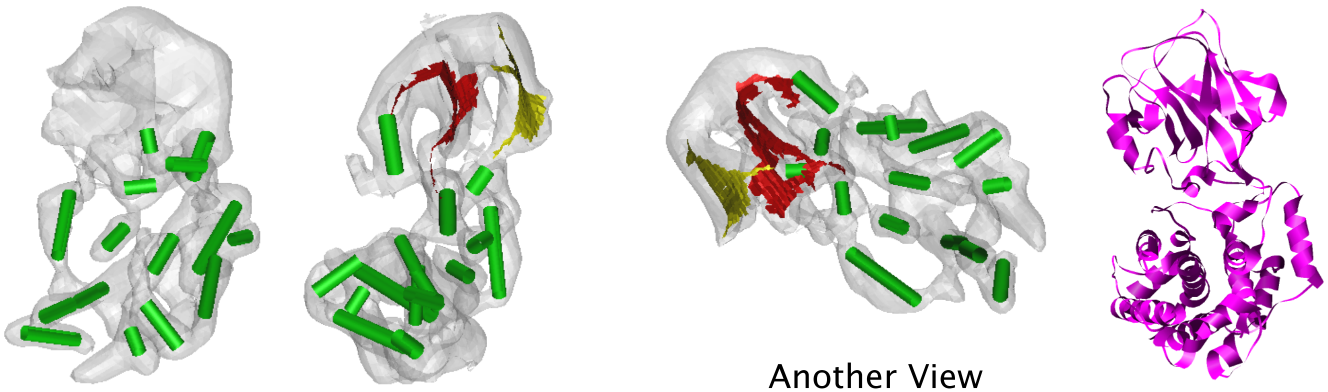

Helices | Helices and Sheets | Another View | Ribbon Diag. of PDB

α-helices 15/16
β-sheets 3/3

3D EM map of P8 segmented out from cryo-EM map of Rice Dwarf Virus (RDV) at 6.8 A resolution

Center for Computational Visualization http://www.ices.utexas.edu/CCV
Institute of Computational and Engineering Sciences
Department of Computer Sciences University of Texas at Austin

August 2007

#5B(I)b:Tertiary Structure Elucidation

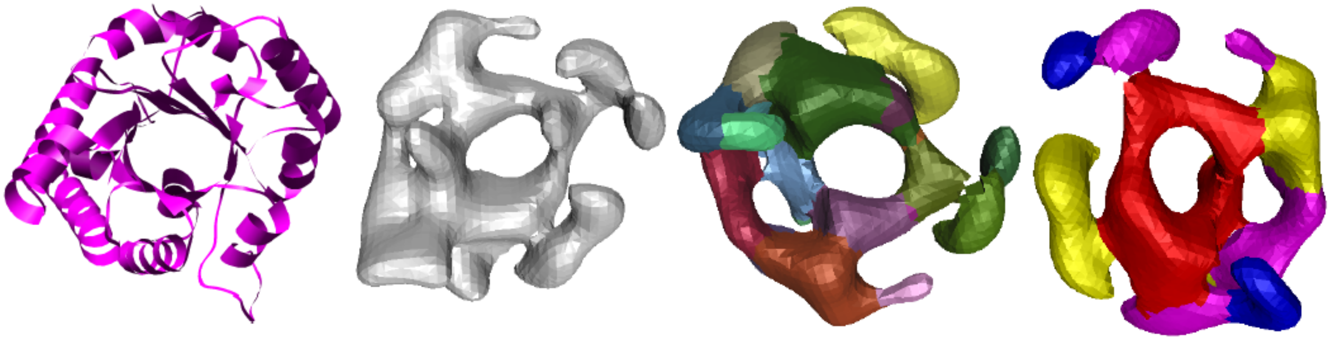

Step 1: Vor/Del(P) computation (using *CGAL*).

Step 2: Identification of Interior Medial Axis M

Step 3:

3.a: Identification of Critical points of h_P from Vor/Del(P).

3.b: Selection of Critical points only on M.

[By DGRS2005, Critical points are either near S or near M

- Step 4: Decomposition of shape via S3 stable manifold of maxima on M
- Step 5: Width Test to select the subsets of S3 .

Tertiary Structure Elucidation

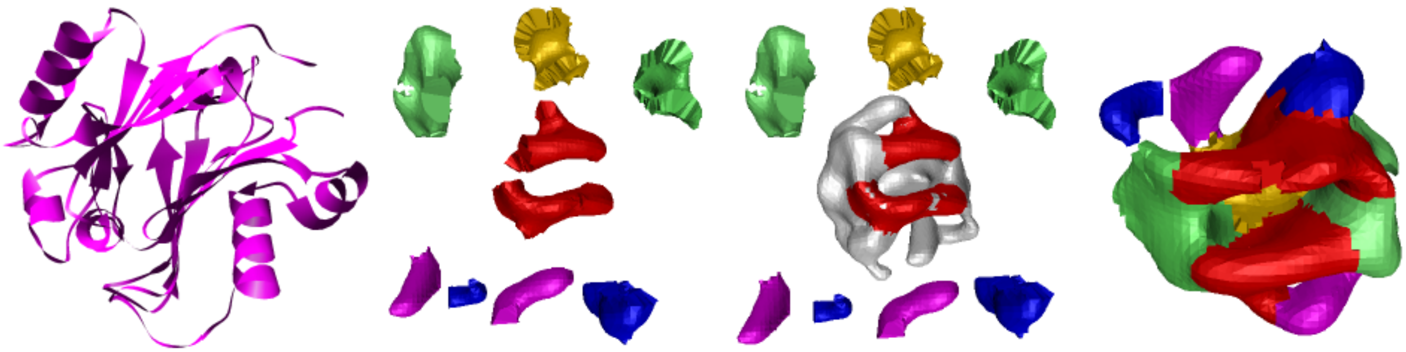

(a) (b) (c) (d)

1AOR (12Å)

The tertiary fold of 1AOR is a β-sandwich (two red sheets), which is surrounded by the differently colored helical segments.

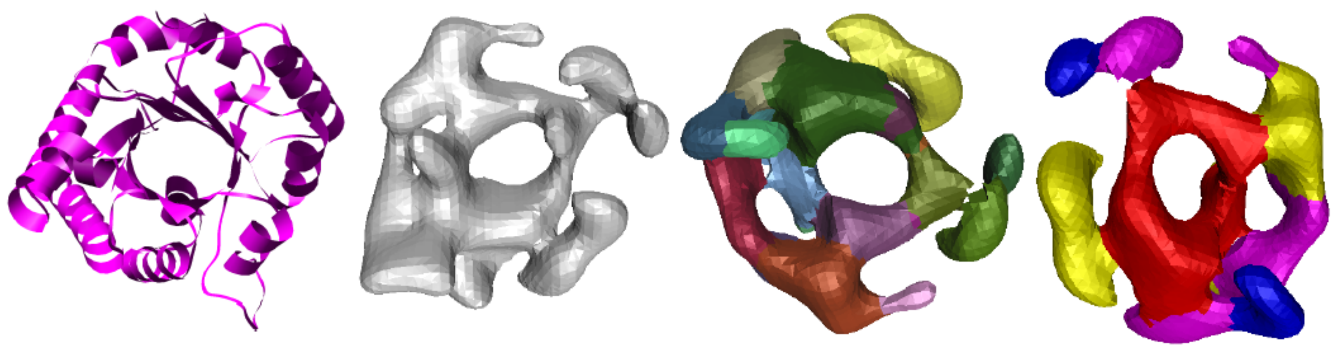

The tertiary fold of 1TIM is .a α/β-barrel.

The β -region in the middle is segmented as red while the helical segments surrounding it are colored differently.

Modeling Human Joint Dynamics and Stress

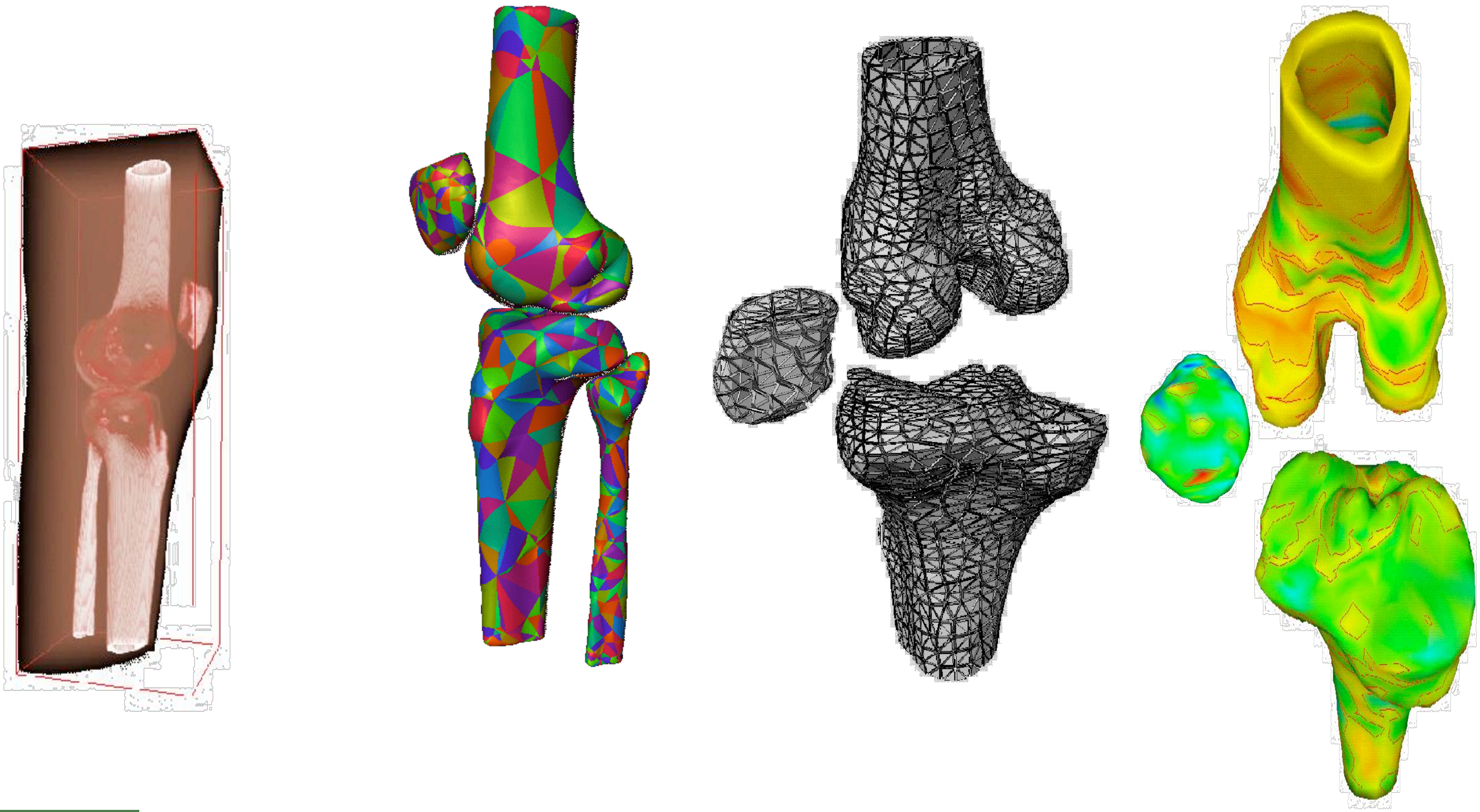

Center for Computational Visualization
Institute of Computational and Engineering Sciences
Department of Computer Sciences
University of Texas at Austin

Non-Linear Algebraic Curve and Surface Finite Elements ?

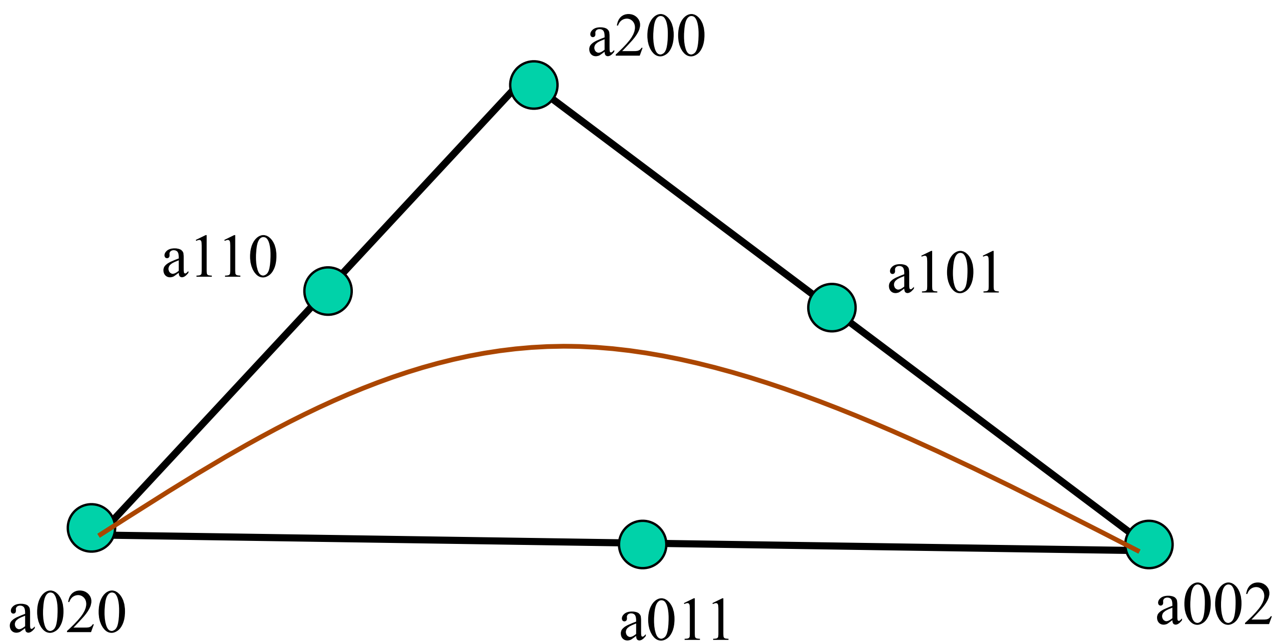

The conic curve interpolant is the zero of the bivariate quadratic polynomial interpolant over the triangle

A-spline segment over BB basis

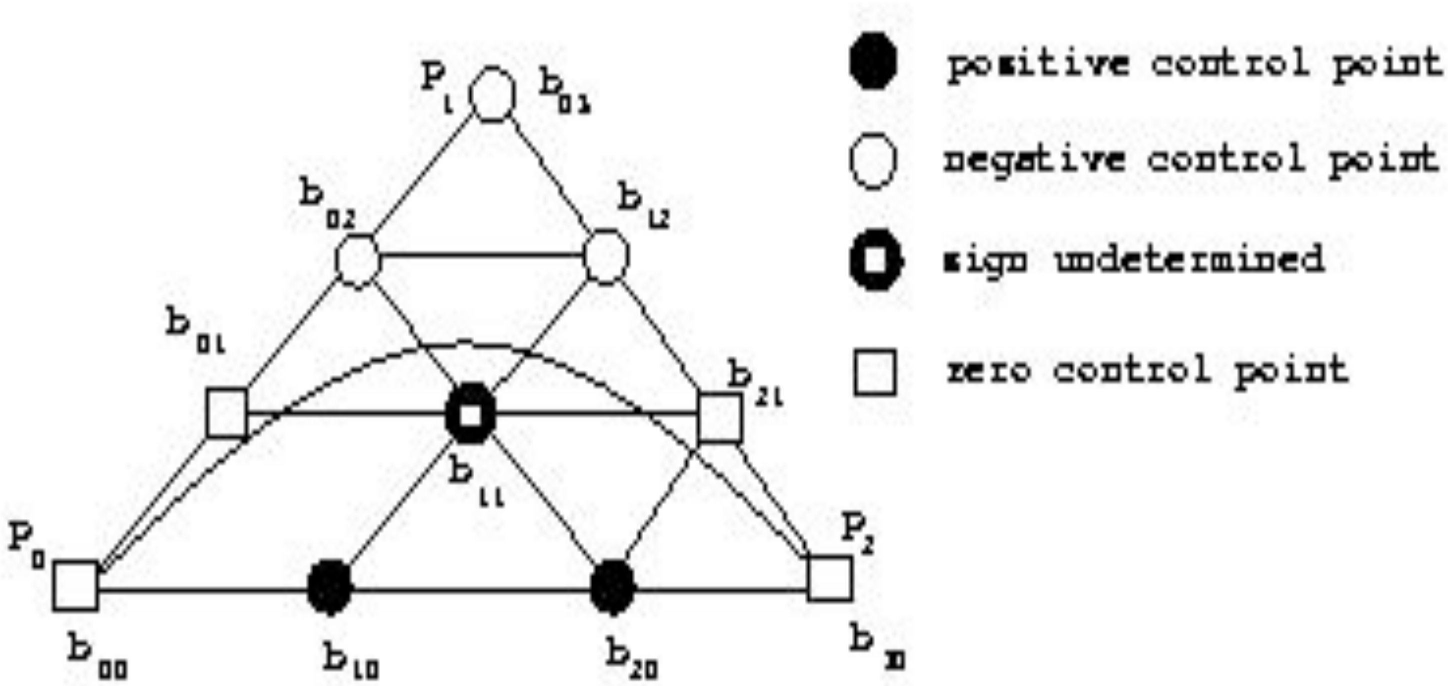

Examples of Discriminating Curve Families

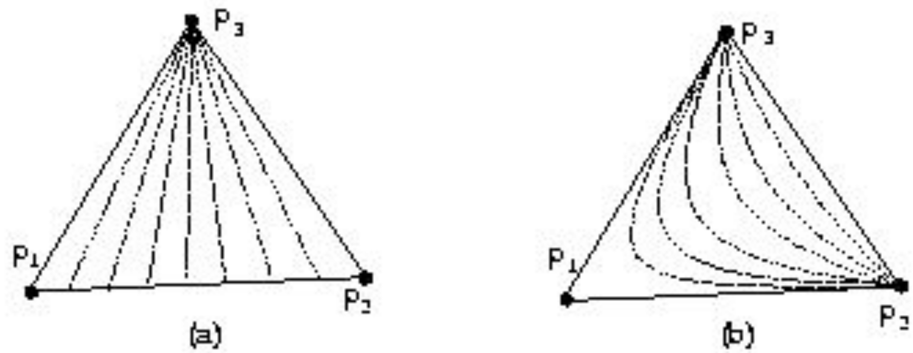

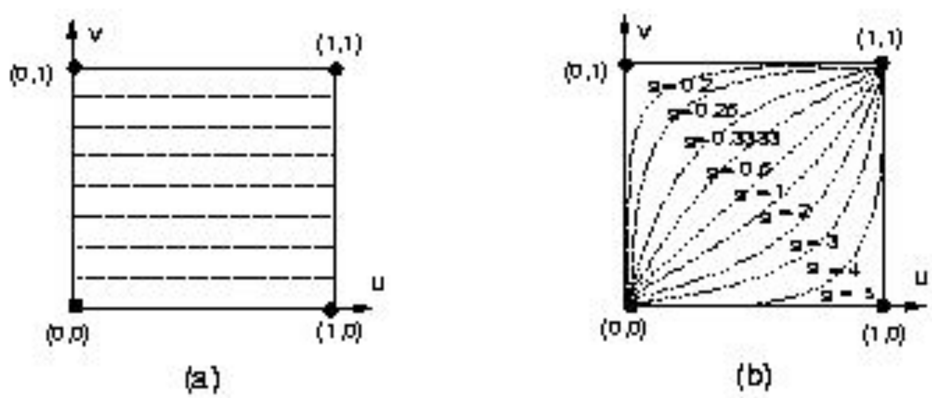

Regular A-spline Segments

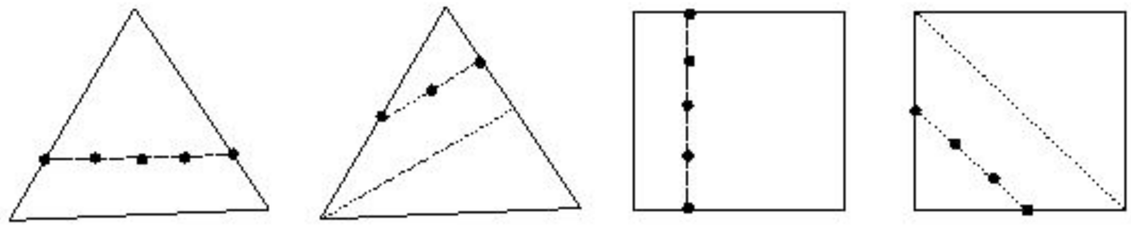

For a given discriminating family D(R, R_1, R_2), let f(x, y) be a bivariate polynomial . If the curve f(x, y) = 0 intersects with each curve in D(R, R_1, R_2) only once in the interior of R, we say the curve f = 0 is regular(or A-spline segment) with respect to D(R, R_1, R_2).

If $B_0(s)$, $B_1(s)$, … has one sign change, then the curve is

(a) D_1 - regular curve.

(b) D_2 - regular curve.

(c) D_3 - regular curve.

(d) D_4 - regular curve.

Constructing Scaffolds

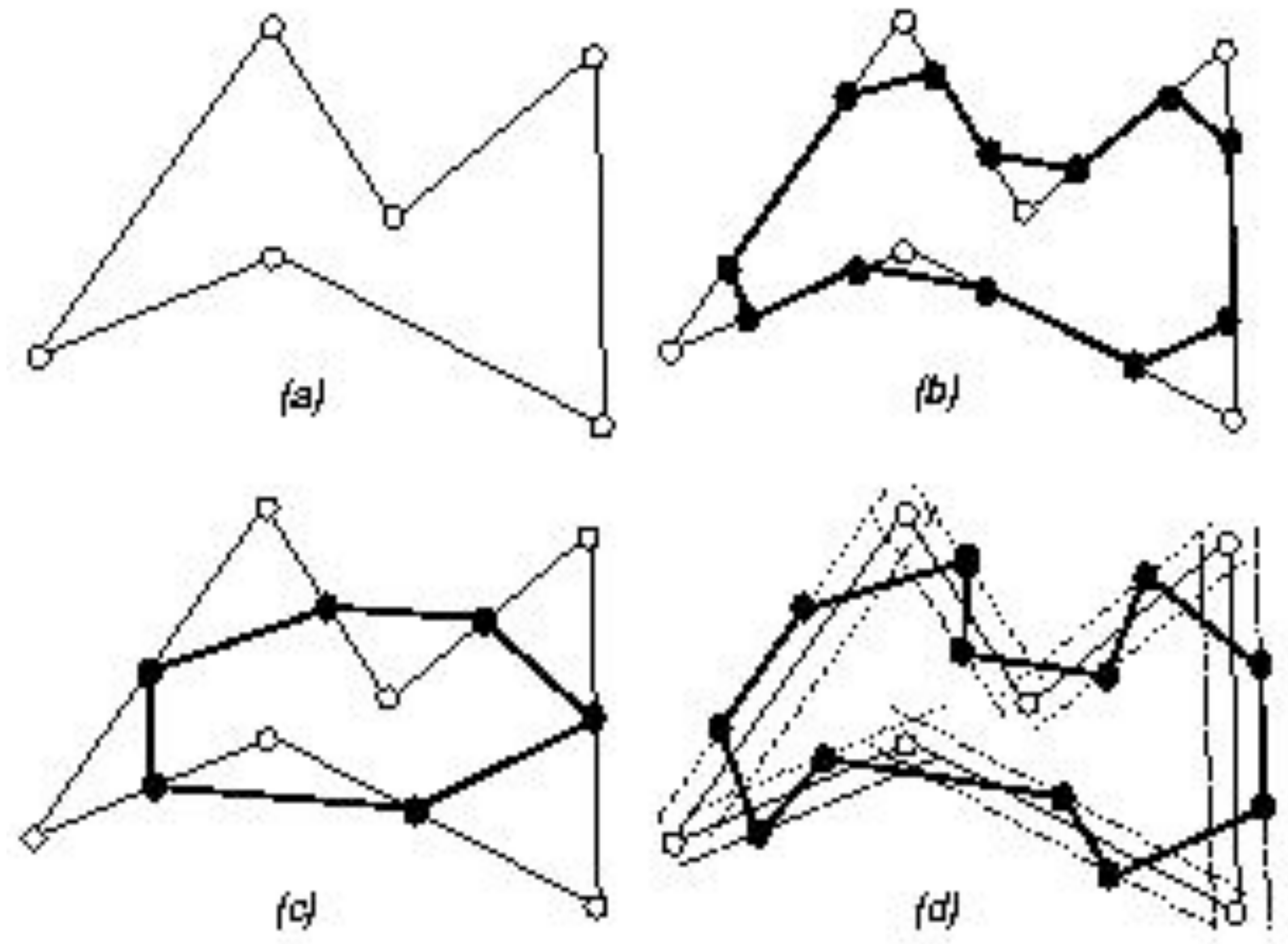

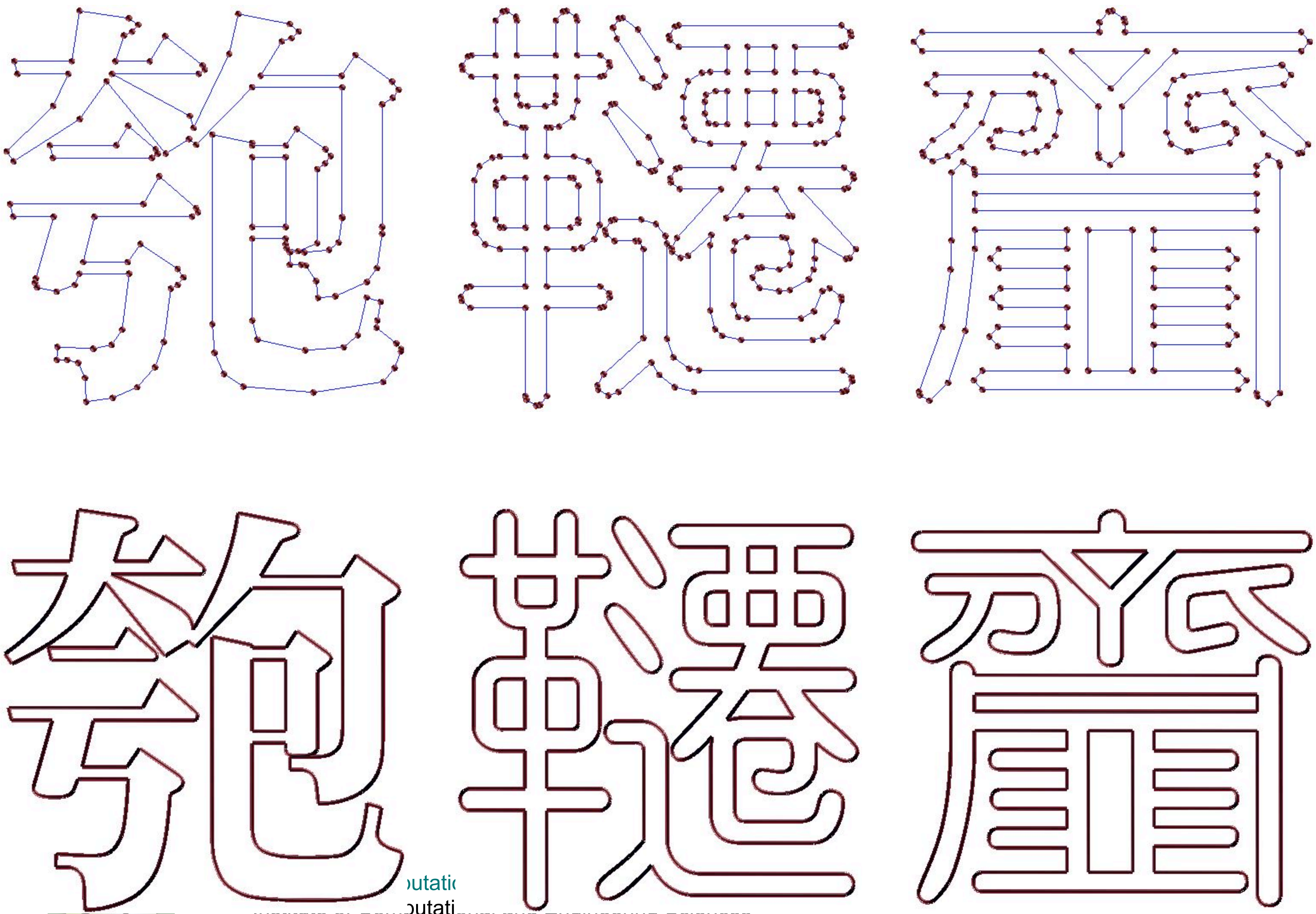

A-patch Surface (C^1) Interpolant

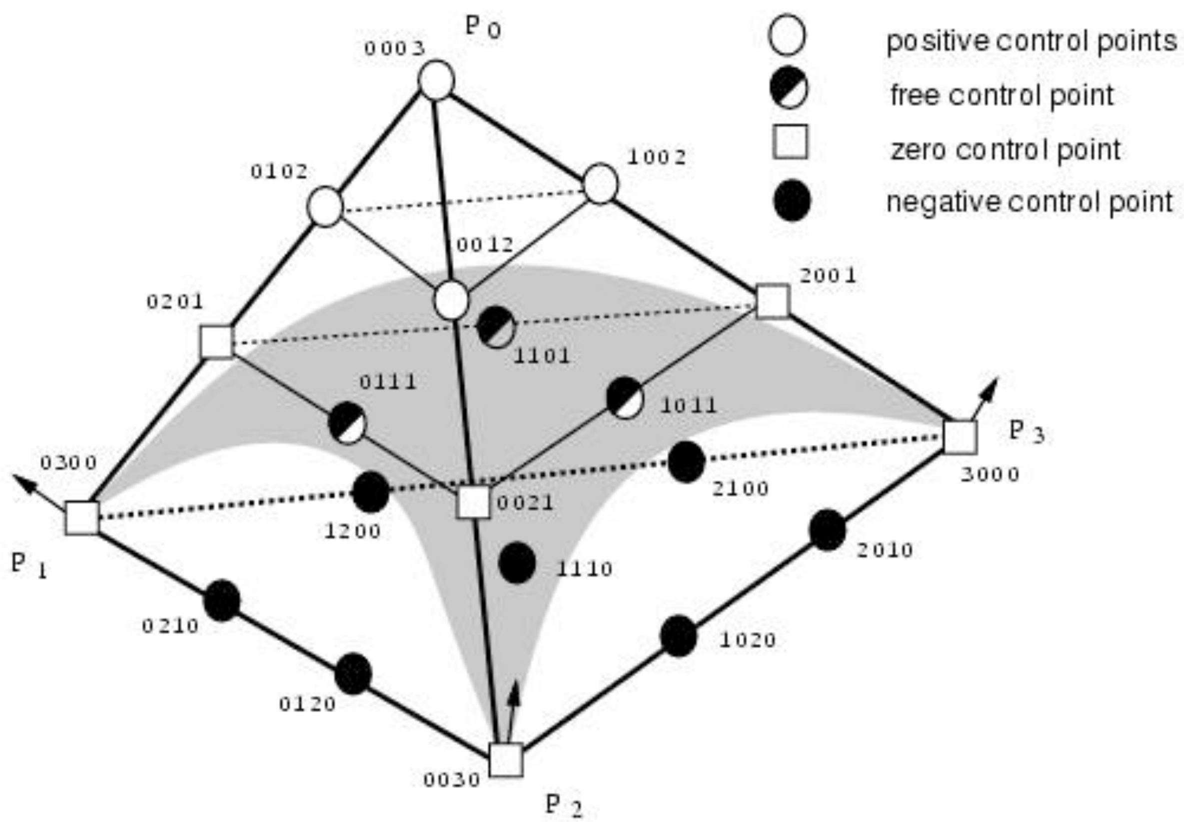

- An implicit single-sheeted polynomial interpolant on a tetrahedron

A-Patches

- Given tetrahedron vertices $p_i=(x_i,y_i,z_i)$, $i=1,2,3,4$, α is barycentric coordinates of $p=(x,y,z)$:

$$\begin{bmatrix} x \\ y \\ z \\ 1 \end{bmatrix} = \begin{bmatrix} x_1 & x_2 & x_3 & x_4 \\ y_1 & y_2 & y_3 & y_4 \\ z_1 & z_2 & z_3 & z_4 \\ 1 & 1 & 1 & 1 \end{bmatrix} \begin{bmatrix} \alpha_1 \\ \alpha_2 \\ \alpha_3 \\ \alpha_4 \end{bmatrix}$$

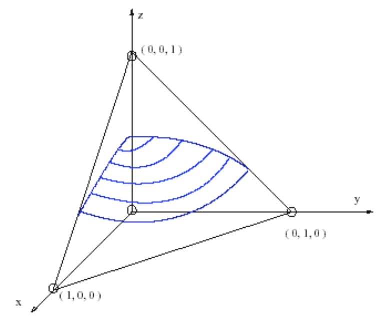

- function $f(p)$ of degree n can be expressed in Bernstein-Bezier form :

$$f(p) = \sum_{|\lambda|=n} b_\lambda \, B^n_\lambda(\alpha), \;\; \lambda \in \mathcal{Z}^4_+ \qquad B^n_\lambda(\alpha) = \frac{n!}{\lambda_1!\lambda_2!\lambda_3!\lambda_4!} \, \alpha_1^{\lambda_1} \alpha_2^{\lambda_2} \alpha_3^{\lambda_3} \alpha_4^{\lambda_4}$$

- Algebraic surface patch(A-patch) within the tet is defined as $f(p)=0$.

Algebraic Patches: Smooth Boundary Elements

- Implicit form of Isocontour : $f(x,y,z) = w$

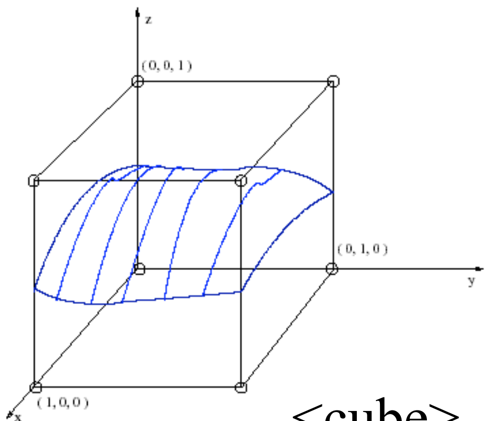

<cube>

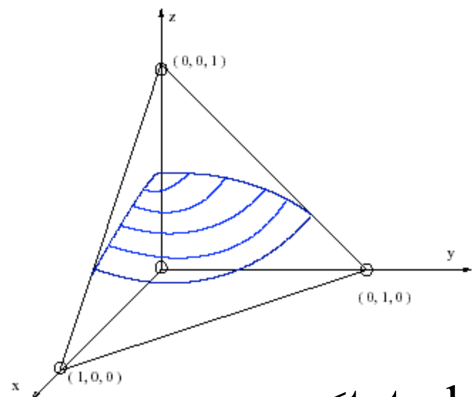

<tetrahedron>

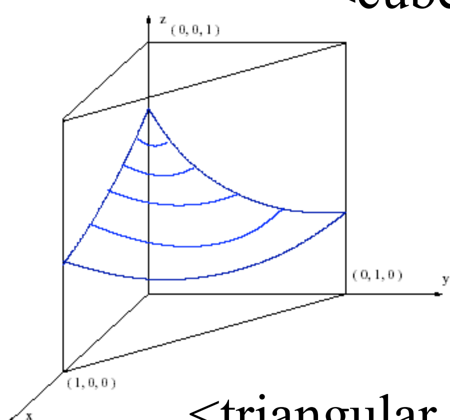

<triangular prism>

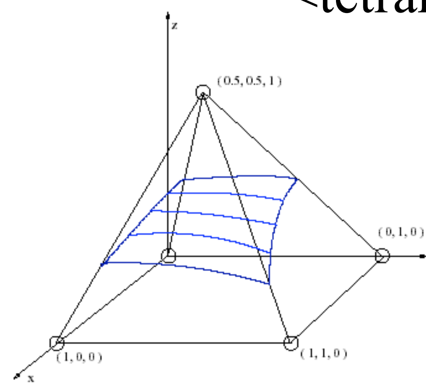

<square pyramid>

A-patch Contouring

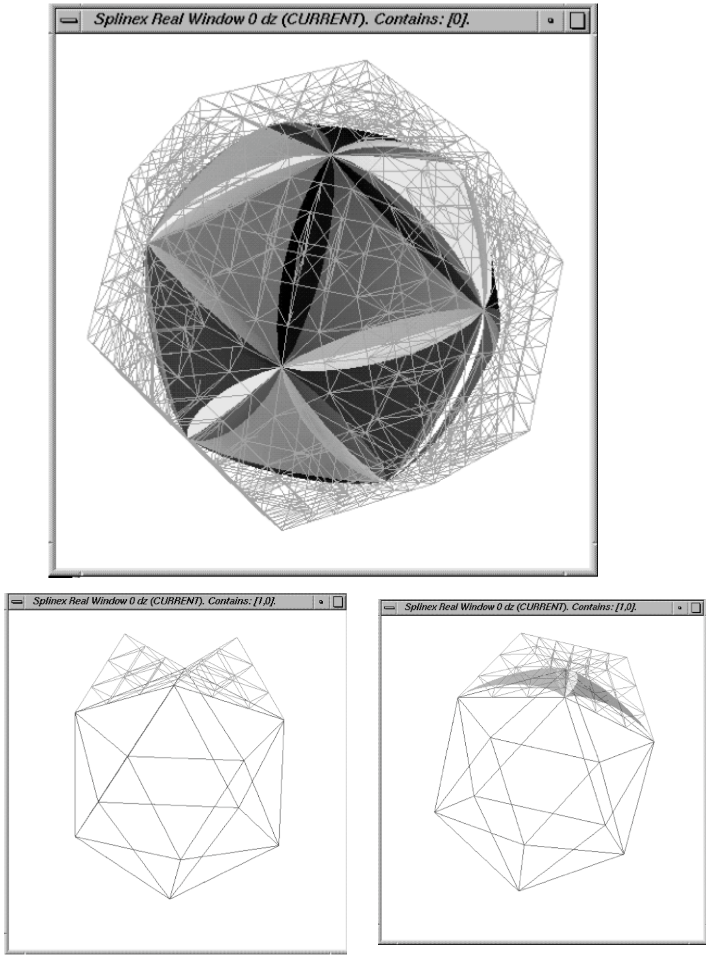

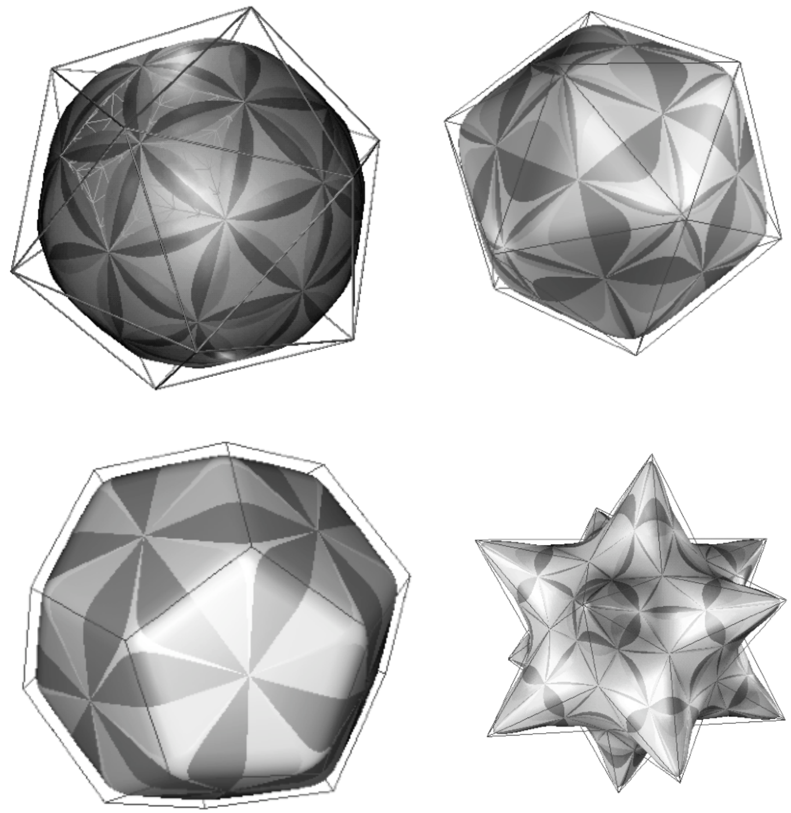

Center for Computational Visualization
Institute of Computational and Engineering Sciences
Department of Computer Sciences
University of Texas at Austin

October 2007

A-patches [Bajaj, Chen, Xu 1994]

- Zero contour of a trivariate polynomial: f(x,y,z)=0
- Single-sheeted patches
- C^1 smoothing of arbitrary polyhedra
- Conversion to Trimmed NURBS

Computing functions on surface

- Surface: Weighted least squares approximation of data points and signed-distance samples
- Function:Weighted least squares approximation of function values

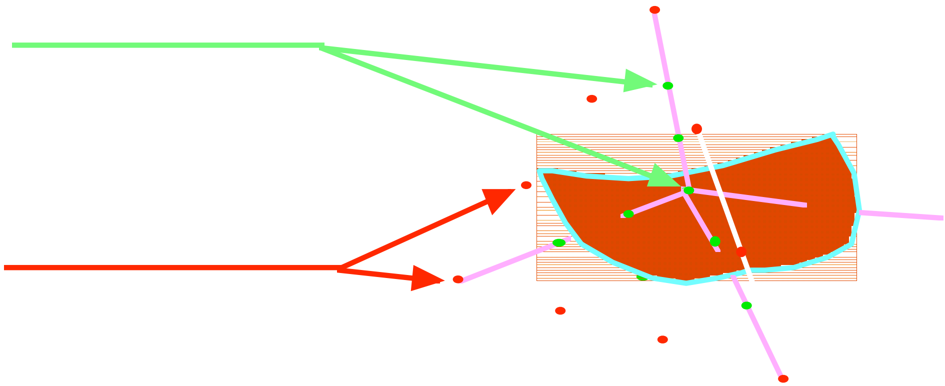

A-patch Contouring

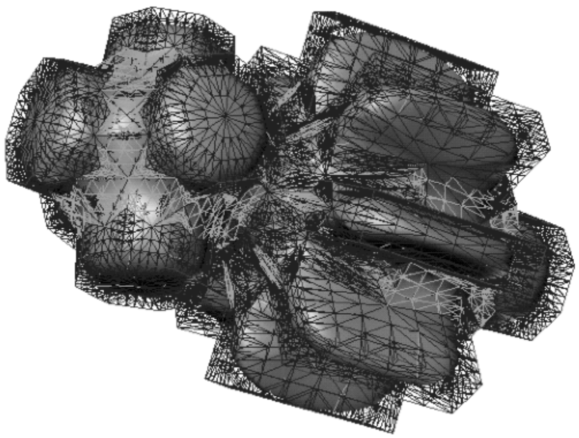

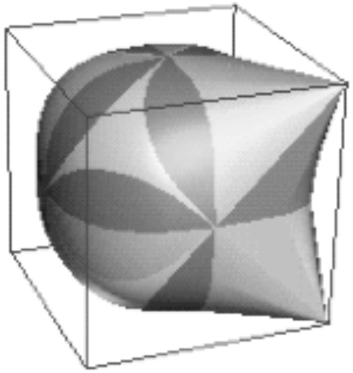

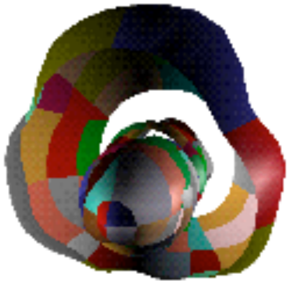

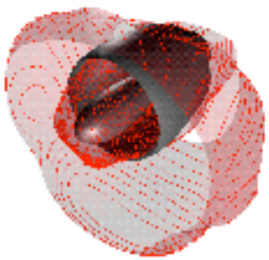

A-Patch Approximation

- ~9200 points, 406 patches (degree 3), 1% error

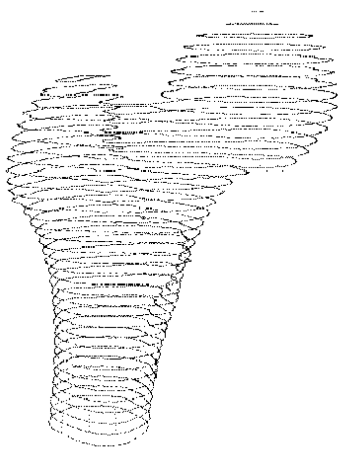

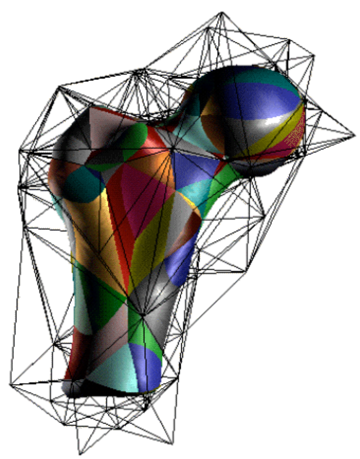

Automatic CAD Model (features) Reconstruction from Point Clouds

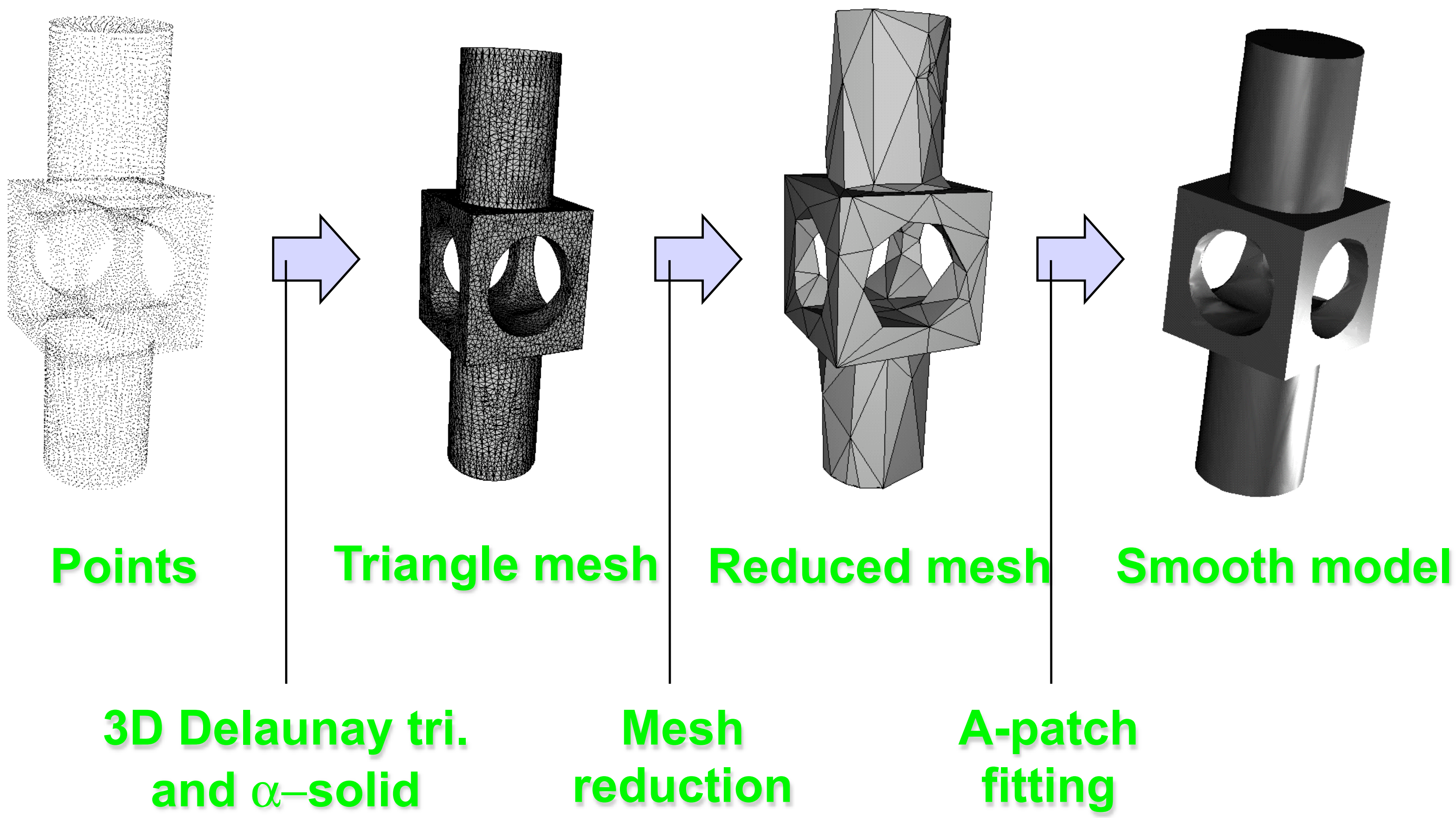

Sculpturing

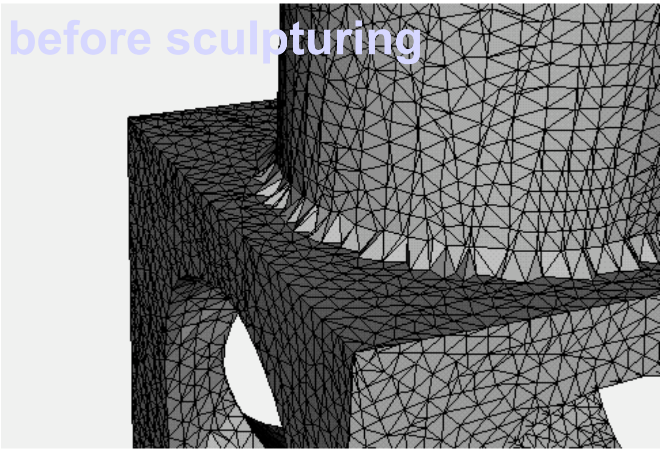

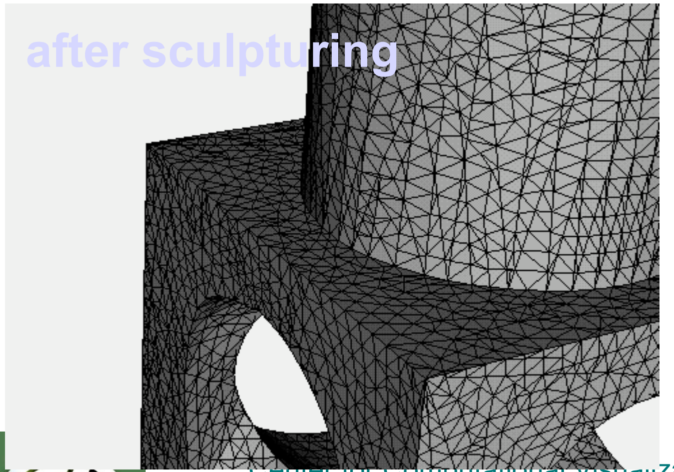

α -solid is refined by iteratively removing tetrahedra adjacent to the boundary, based on two principles:

– remove if a data point is occluded

– remove if sum of dihedral angles decreases

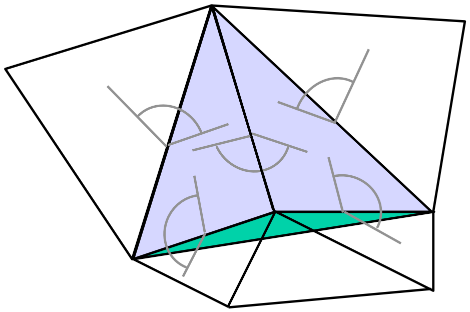

Dihedral angles formed by boundary faces

Mesh reduction

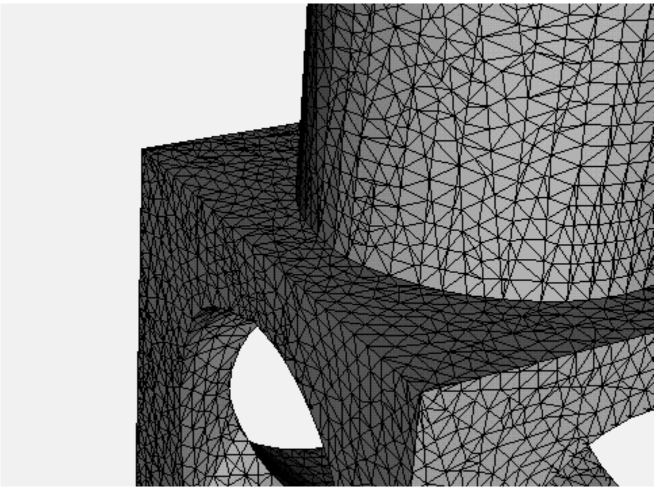

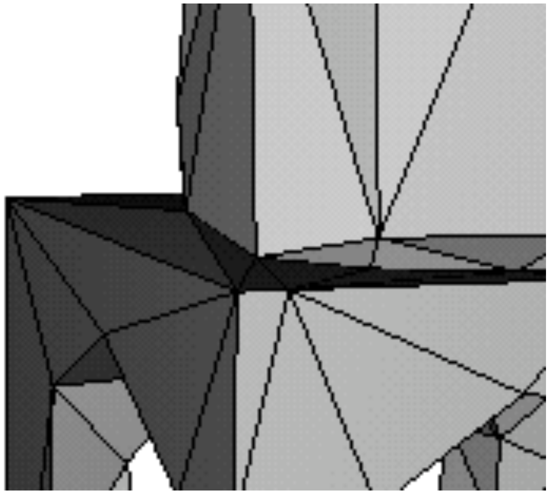

- *Mesh reduction technique for triangle meshes with multivariate data*

- Based on incremental deletion of vertices and retriangulation
- Guaranteed, global error-bound
- Sharp feature recognition and preservation

Surface Fitting

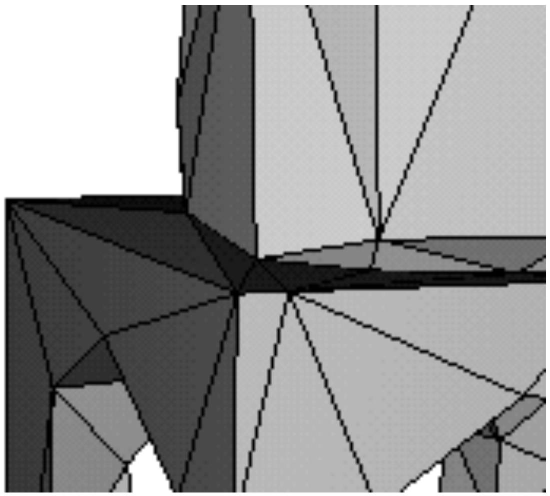

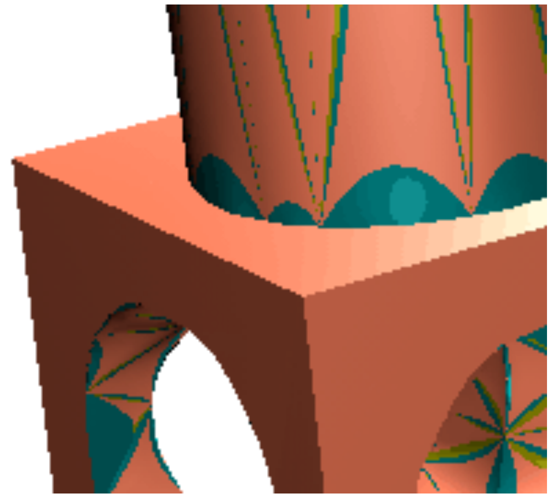

- Uses cubic A-patches (algebraic patches)
- C^1 continuity

- Sharp features (corners, sharp curved edges)
- Singularities

Further Reading: Point-set Surface Reconstruction

1. Boissonnat, J. D., 1984, "Geometric Structures for Three Dimensional Shape Representation," ACM Transact. on Graphics, 3(4), pp 266–286.
2. Edelsbrunner, H., and Mucke, E. P., 1994, "Three-dimensional Alpha Shapes," ACM Trans. Graphics, 13, pp 43–72.
3. Bajaj, C., Bernardini, F., and Xu, G., 1995, "Automatic Reconstruction of Surfaces and Scalar Fields from 3D Scans," ACM SIGGRAPH, pp. 109–118.
4. Amenta, N., Bern, M., and Kamvysselis, M., 1998, "A New Voronoi-based Surface Reconstruction Algorithm," ACM SIGGRAPH, pp 415-421.
5. Amenta, N., Choi, S., Dey, T. K., and Leekha, N., 2002, "A Simple Algorithm for Homeomorphic Surface Reconstruction," Internat. J. Comput. Geom. & Applications, 12, pp. 125-141.
6. Boissonnat, J. D., and Cazals, F., 2000, "Smooth Surface Reconstruction via Natural Neighbor Interpolation of Distance Functions," Proc. 16th. Annu. Sympos. Comput. Geom., pp 223–232.
7. Amenta, N., Choi. S., and Kolluri, R. K., 2001, "The Power Crust," Proc. 6th Annu. Sympos. Solid Modeling Applications, pp. 249-260.
8. Dey T. K. and Goswami S., 2003, "TightCocone: A Watertight Surface Reconstructor," Proc. 8th Annu. Sympos. Solid Modeling Applications, pp. 127-134.
9. Dey T. K. and Goswami S., 2003, "Provable Surface Reconstruction from Noisy Samples," Proc. 20th Annu. Sympos. Comp. Geom., pp. 330-339.
10. Hoppe, H., DeRose, T., Duchamp, T., McDonald, J., and Stuetzle, W., 1992, "Surface Reconstruction from Unorganized Points," ACM SIGGRAPH 92, pp 71-78.
11. Curless, B., and Levoy, M., 1996, "A Volumetric Method for Building Complex Models from Range Images," ACM SIGGRAPH, pp 303-312.

Further Reading: Medial Axis Transform (MAT)

- H. Edelsbrunner and N. Shah. Triangulating topological spaces. Proc. 10th ACM Sympos. Comput. Geom., (1994), 285-292.
- T. K. Dey and W. Zhao. Approximate medial axis as a Voronoi subcomplex. Proc. 7th ACM Sympos. Solid Modeling Appl., 2002, 356--366.
- Nina Amenta and Ravi Krishna Kolluri, "The medial axis of a union of balls", Computational Geometry 2001‟ 20(1-2) pages "25-37",
- F. Chazal, A. Lieutier, The Lambda Medial Axis, Graphical Models, Volume 67, Issue 4 , July 2005, Pages 304-331
- André Lieutier: Any open bounded subset of has the same homotopy type as its medial axis. Computer-Aided Design 36(11): 1029-1046 (2004)
- Joachim Giesen, Edgar A. Ramos, Bardia Sadri: Medial axis approximation and unstable flow complex. Symposium on Computational Geometry 2006: 327-336

Further Reading: A-splines & A-patches

1. G. Xu, C. Bajaj, S. Evans
   C1 Modeling with Hybrid Multiple-sided A-patches
   Special issue on Surface and Volume Reconstructions in the International Journal of Foundations of Computer Science, 13, 2, 261-284.
2. C. Bajaj, G. Xu, R. Holt, A. Netravali
   Hierarchical Multiresolution Reconstruction of Shell Surfaces
   Computer Aided Geometric Design, 19:2(2002), 89-112.
3. G. Xu, C. Bajaj, H. Huang
   C1 Modeling with A-patches from Rational Trivariate Functions
   Computer Aided Geometric Design, 18:3(2001), 221-243.
4. C. Bajaj, G. Xu
   Regular Algebraic Curve Segments (III) - Applications in Interactive Design and Data Fitting
   Computer Aided Geometric Design, 18:3(2001), 149-173.
5. C. Bajaj, G. Xu
6. **Smooth Shell Construction with Mixed Prism Fat Surfaces**
   Brunett, G., Bieri,H., Farin, G. (eds.), Geometric Modeling Computing Supplement, 14, (2001), 19-35.
7. G. Xu, C. Bajaj, W. Xue
   Regular algebraic curve segments (I)-Definitions and characteristics
   Computer Aided Geometric Design, 17:6(2000), 485-501.
8. G. Xu, C. Bajaj, C. Chu
   Regular Algebraic Curve Segments (II) - Interpolation and Approximation
   Computer Aided Geometric Design, 17:6(2000), 503-519
9. C. Bajaj, G. Xu
   A-Splines: Local Interpolation and Approximation Using Gk- Continuous Piecewise Real Algebraic Curves
   Computer Aided Geometric Design, 16:6(1999), 557-578.